RSC Advances

PAPER

View Article Online
View Journal | View Issue

Cite this: *RSC Adv.*, 2024, **14**, 4654

Semi-synthesis, α-amylase inhibition, and kinetic and molecular docking studies of arylidene-based sesquiterpene coumarins isolated from *Ferula tunetana* Pomel ex Batt†

Wiem Baccari,[a] Ilyes Saidi,[a] Insaf Filali,*[b] Mansour Znati,[a] Houda Lazrag,[c] Moncef Tounsi,[d] Axel Marchal,[ef] Pierre Waffo-Teguo[ef] and Hichem Ben Jannet *[a]

Received 4th November 2023
Accepted 13th January 2024

DOI: 10.1039/d3ra07540k

rsc.li/rsc-advances

Despite all the significant progresses made to enhance the efficacy of the existing bank of drugs used to manage and cure type II diabetes mellitus, there is still a need to search and develop novel bioactive compounds with superior efficacy and minimal adverse effects. This study describes the valorization of the natural bioactive sesquiterpene coumarin *via* the semi-synthesis of new analogs and the study of their α-amylase inhibition activity. The sesquiterpene coumarin named coladonin (**1**) was quantitatively isolated from the chloroform extract of endemic *Ferula tunetana* roots. Subsequently, the oxidation of **1** *via* the Jones oxidation reaction, used as a key reaction, afforded precursor **2**. The condensation of oxidized coladonin (**2**) with various aryl aldehydes provided a series of new arylidene-based sesquiterpene coumarin derivatives (**3a–m**), which were characterized by NMR and ESI-HRMS experiments. All derivatives evaluated *in vitro* for their α-amylase inhibitory potential showed interesting α-amylase inhibition with IC_{50} values ranging from 7.24 to 28.98 μM. Notably, compounds **3k** and **3m** exhibited lower IC_{50} values (7.24 μM and 8.38 μM, respectively) compared to the standard (acarbose: IC_{50} = 9.83 μM). In addition, the structure–activity relationship (SAR) for all the compounds was studied. The most active compounds were found to be mixed-type inhibitors, which was revealed by kinetic studies. Furthermore, molecular *in silico* docking studies were established for all synthesized analogs with the binding site for the α-amylase enzyme.

1 Introduction

According to the WHO, with more than 578 million cases expected worldwide by 2030, diabetes mellitus (DM) is considered the most chronic metabolic disease having a high mortality rate and huge health costs.[1,2] DM is characterized by abnormal blood-glucose levels (hyperglycemia) due to the developed insulin resistance (T2DM) and/or insufficient secretion of insulin (T1DM), as well as other complications such as nephropathy.[3,4] One of the main approaches to managing DM involves inhibiting the α-amylase enzyme, which is responsible for cleaving carbohydrates (starch and oligosaccharides) into small sugar units, ultimately leading to hyperglycemia and the subsequent development of diabetes.[5] In this regard, the inhibition of the α-amylase enzyme plays an important role in the treatment of diabetes. In fact, targeting α-amylase inhibitors with small molecules is one of the methods to find new antidiabetic drugs.[6,7] In recent years, there has been increasing interest in the use of natural products as potential antidiabetic therapeutic agents.[8–10]

Traditional medicines involve the utilization of plants belonging to the Apiaceae family, especially the genus *Ferula* (170 species),[11] in the treatment of various diseases. Different parts of *Ferula* (the extracts of *F. persica*, *F. mongolica*, *F. sinaica* and *F. ferulago*) have a reputation in the treatment of diabetic diseases.[12] In Tunisia, only one endemic species of the *Ferula* genus has been identified: *F. tunetana* Pomel ex Batt.[13] The phytochemical features of the roots of *F. tunetana* include the

[a]*University of Monastir, Faculty of Science of Monastir, Laboratory of Heterocyclic Chemistry, Natural Products and Reactivity (LR11ES39), Team: Medicinal Chemistry and Natural Products, Avenue of Environment, 5019 Monastir, Tunisia. E-mail: hichem.bjannet@gmail.com*

[b]*Department of Chemistry, College of Science and Humanities in Al-Kharj, Prince Sattam bin Abdulaziz University, Al-Kharj 11942, Saudi Arabia*

[c]*University of Monastir, Higher Institute of Biotechnology of Monastir, Laboratory of Genetics, Biodiversity and Bioresources Valuation LR11S41, 5019 Monastir, Tunisia*

[d]*Preparatory Year Deanship, Basic Science Department, Prince Sattam Bin Abdulaziz University, Alkharj 11942, Saudi Arabia*

[e]*Université de Bordeaux, Institut des Sciences de la Vigne et du Vin, EA 4577, Unité de Recherche Œnologie 210 Chemin de Leysotte, CS50008, 33882 Villenave d'Ornon, France*

[f]*Université de Bordeaux, Bordeaux INP, Bordeaux Sciences Agro, UMR 1366 OENOLOGIE, ISVV, 33140 Villenave d'Ornon, France*

† Electronic supplementary information (ESI) available. See DOI: https://doi.org/10.1039/d3ra07540k

presence of various compounds, particularly sesquiterpene coumarins (six compounds) including tunetacoumarin A, coladin, coladonin (major compound), isosamarcandin angelate, 13-hydroxyfeselol, and umbelliprenin.[14] The same work reported the significant cytotoxic activity of coladonin (the major compound) against two human colon cancer cell lines: HT-29 and HCT-116. Sesquiterpene coumarins, which consist of a coumarin moiety attached to a sesquiterpene moiety, are almost exclusively found in the roots of the genus *Ferula*.[15] In fact, sesquiterpene coumarins are the most important owing to their wide range of promising biological properties. Numerous studies have shown that this type of natural products exhibit excellent anti-diabetic effects (Fig. 1).[16,17]

Recently, numerous studies have demonstrated that the pharmacophore arylidene fragment has attracted significant attention due to its broad spectrum of pharmacological and biological effects. Similarly, arylidenes are known as antidiabetic agents (Fig. 2).[18,19] Moreover, interest in α,β-unsaturated ketones has heightened in drug discovery, as they hold promise for pharmaceutical applications. In particular, the antidiabetic drug Epalrestat is among the remarkable compounds derived from α,β-unsaturated ketones (G in Fig. 2).[20]

Encouraged by the significant antidiabetic potential of sesquiterpene coumarins, arylidene and α,β-unsaturated ketones, and with the aim of accessing new arylidene compounds, we sought to exploit coladonin (**1**) isolated in sufficient quantity from the roots of *F. tunetana* to prepare a new series of structural analogs of arylidenes (Fig. 3).

The evaluation of the α-amylase inhibition of all the synthesized compounds was studied and is reported herein. The mechanism inhibition of the most active compounds was determined *via* a kinetic study. Furthermore, the structure–activity relationship (SAR) was *in silico* approved by the molecular docking analysis.

2 Results and discussion

2.1. Chemistry

Coladonin (**1**) was isolated from the $CHCl_3$ extract of *F. tunetana* roots. It was identified with the help of its spectroscopic data (NMR spectra (^{1}H, HSQC and HMBC)) and by comparison with the reports in the literature.[11] Indeed, analysis of the ^{1}H NMR and HSQC spectra of this compound reveals, among other correlations, the presence of the correlation cross-peaks H-3 (δ_H 6.25)/C-3 (δ_c 113.3), H-4 (δ_H 7.64)/C-4 (δ_c 143.8), H-5 (δ_H 7.36)/C-5 (δ_c 129.0), H-6 (δ_H 6.83)/C-6 (δ_c 113.4) and H-8 (δ_H 6.82)/C-8 (δ_c 101.6), suggesting the presence of the umbelliferone skeleton, previously identified in the roots of this plant.[14] The remaining signals are assigned through HSQC, COSY, HMBC, and ROESY experiments to a sesquiterpene, confirming that compound (**1**) is a derivative of the sesquiterpene-coumarin nature. Indeed, the complete analysis of all 1D and 2D NMR spectra, supported by bibliographic data on sesquiterpene-coumarins previously isolated from this plant, allowed us to propose the structure of coladonin. The absolute configurations were deduced from dipolar correlations observed in the ROESY spectrum between H-3′/H-13′, H-3′/H-5′, H-5′/H-9′, and H-11′/H-15′, indicating the β orientation of protons H-3′, H-5′, H-9′, and methyl 13′, and the α orientation of the methylene (CH_2)-11′, as well as methyl 14′ and 15′.

In our approach to access to the desired compounds **3a–m**, we started first by the oxidation of the coladonin (**1**), *via* the Jones oxidation reaction. The oxidized coladonin (**2**) was obtained in good yields (92%) (Scheme 1).

The structure of compound **2** was established according to its spectral data (NMR spectra (^{1}H, HSQC and HMBC) and ESI-HRMS) (Fig. 4). Indeed, the ^{1}H NMR spectrum of compound **2** showed the absence of the signal at δ_H 3.31 related to the H-3′ proton compared to the ^{1}H NMR spectrum of coladonin (**1**). The ^{13}C NMR confirmed the oxidation of the secondary alcohol at C-3′ by the observation of a new signal at δ_C 215.9 attributable to the carbonyl group.

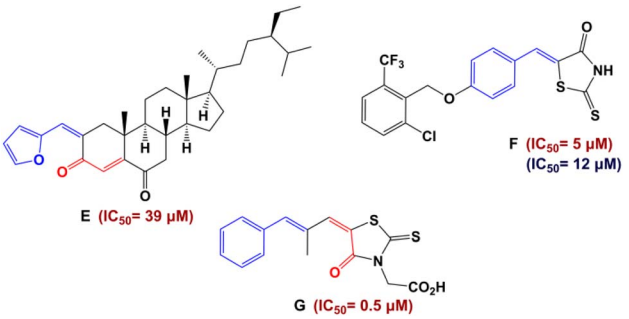

Fig. 2 Structures of antidiabetic arylidene and α,β-unsaturated ketone derivatives. Red color indicates IC_{50} values against α-glucosidase and blue color IC_{50} values against α-amylase.

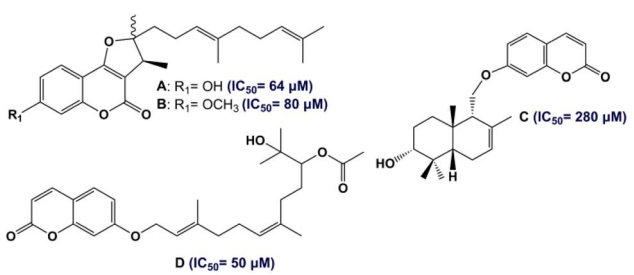

Fig. 1 Structures of antidiabetic (anti-α-glucosidase) sesquiterpene coumarins.

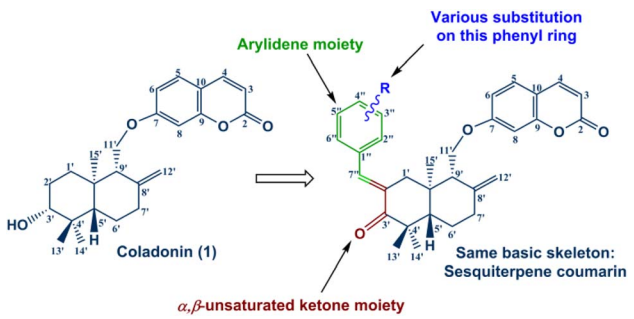

Fig. 3 General structure of the new sesquiterpene-coumarin arylidenes.

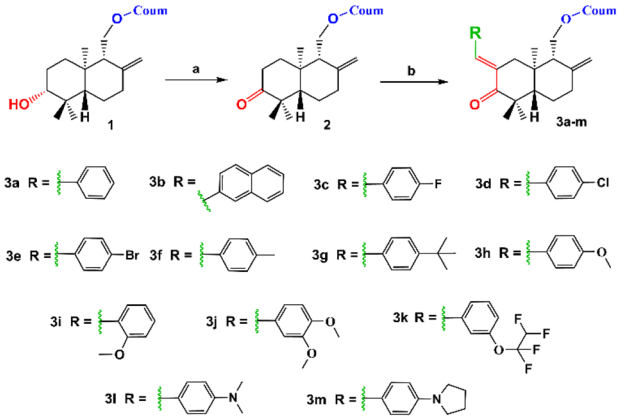

Scheme 1 Synthetic route of **3a–m** derivatives. (a) Jones reagent, acetone, 0–5 °C, 3 h and (b) RCHO, KOH, ethanol, RT, 24 h.

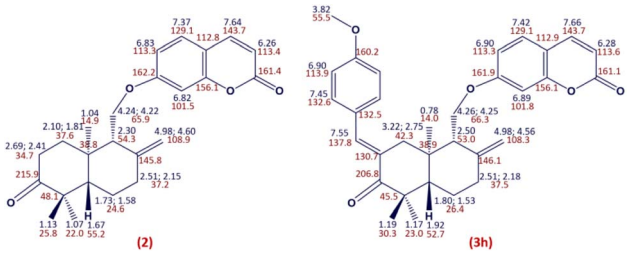

Fig. 4 ^{1}H (blue) and ^{13}C (red) NMR chemical shift assignments for compounds **2** and **3h**.

α-Methylene ketones constitute an important intermediate for the formation of diverse arylidene derivatives known for their high pharmacological and biological properties.[21–23] This attracted our attention towards the use of the oxidized coladonin (**2**) to synthesize the new target compounds **3a–m** by using the α-methylene ketone function in **2** to attach an arylidene moiety to coladonin.

By application of the CLAISENE-SCHMIDT reaction, the oxidized coladonin (**2**) was reacted with a series of aryl aldehydes at room temperature in ethanol for 24 hours, to give **3a–m** in good yields (72–93%) (Scheme 1). The structures of **3a–m** were established by their spectral data (NMR spectra (^{1}H, HSQC and HMBC) and ESI-HRMS). In fact, the ^{1}H NMR spectra of these derivatives showed, in addition to the signals of the oxidized coladonin **2** moiety, the appearance of a new doublet at δ_H 7.45–7.75 due to ethylenic proton H-7″ and also other signals at δ_H 6.70–7.90 attributable to aromatic protons introduced by the used aryl aldehydes. As an example, consider the compound (**3h**); the analysis of its ^{1}H NMR spectrum primarily revealed the appearance of a doublet at δ_H 7.55 (1H, d, $J = 1.8$ Hz), attributable to the ethylenic proton H-7″. Additionally, two doublets at δ_H 6.90 (2H, d, $J = 8.8$ Hz) and 7.45 (2H, d, $J = 8.8$ Hz) were assigned to the aromatic protons of the *para*-substituted aromatic ring, and a singlet at δ_H 3.82 (3H, s) was identified for the methoxy group protons. The HSQC spectrum confirms these spectral data by revealing a new correlation cross-peak with signals at δ_C 113–138, assigned to the carbons of the methine groups of the used aryl aldehyde (Fig. 4).

The stereochemistry (*E*) of the exocyclic double bond $\Delta^{2',7''}$ thus adopted in compounds **3a–m** was confirmed by ROESY spectra showing a NOE between H-1′ and H-2″,6″-atom (Fig. S1†).

2.2. Evaluation of α-amylase inhibition

Among the therapeutic strategies to reduce hyperglycemia is the retarded glucose absorption by inhibiting the activity of α-amylase.[24,25] Meanwhile, all compounds **1**, **2** and **3a–m** were subjected to the evaluation of their *in vitro* α-amylase inhibition. Acarbose served as a standard in this investigation for comparison. The results are expressed in IC_{50} (μM) and reported in Fig. 5.

According to the results, all compounds (**1**, **2** and **3a–m**) showed promising activity against the α-amylase enzyme with IC_{50} values ranging from 7.24 ± 0.36 to 28.98 ± 0.65 μM. In fact, the derivatives **3k**, **3l** and **3m** (IC_{50} = 7.24 ± 0.36, 10.82 ± 0.60 and 8.83 ± 0.22 μM, respectively), followed by **3c**, **3h**, **3b**, **3i**, **3e** and **3d** (IC_{50} = 13.16 ± 0.73, 13.54 ± 0.54, 14.41 ± 0.30, 14.55 ± 0.30, 15.37 ± 0.29 and 17.17 ± 0.50 μM, respectively), showed the highest inhibition potential. Moreover, compounds **3f**, **3g** and **3a** (IC_{50} = 22.31 ± 0.90, 22.67 ± 0.86 and 28.98 ± 0.65 μM, respectively) exhibited moderate activity. It is notable that parent molecules **1** and **2** did not offer remarkable α-amylase inhibition potential (IC_{50} = 22.08 ± 1.10 and 25.03 ± 0.99 μM, respectively) (Fig. 5).

2.3. Structure–activity relationship (SAR) analysis

It is clear that the α-amylase inhibition potential of the newly synthesized compounds depends on the structural factors in relation to the nature and position of substituents on the phenyl rings attached to the arylidene moiety.

As can be seen in Fig. 6, an unsubstituted phenyl ring attached to the arylidene moiety (**3a**, R = Ph) exhibits a weak inhibition potential (IC_{50} = 28.98 ± 0.65 μM) compared to the other derivatives. However, the compound **3b** with a non-

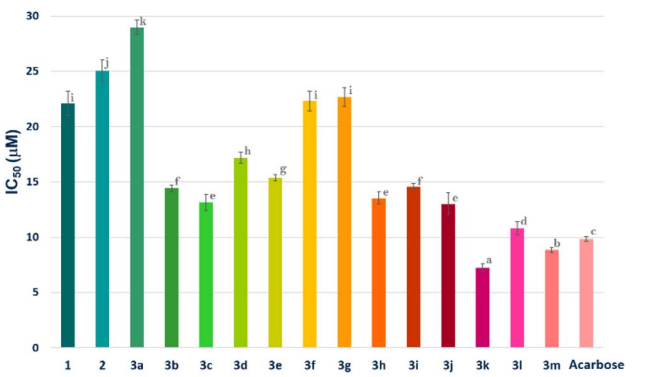

Fig. 5 α-Amylase inhibition (IC_{50} μM) of compounds **1**, **2**, **3a–m** and acarbose. Compounds with the same letter do not have significantly different IC_{50} values at a *p*-value less than 0.05.

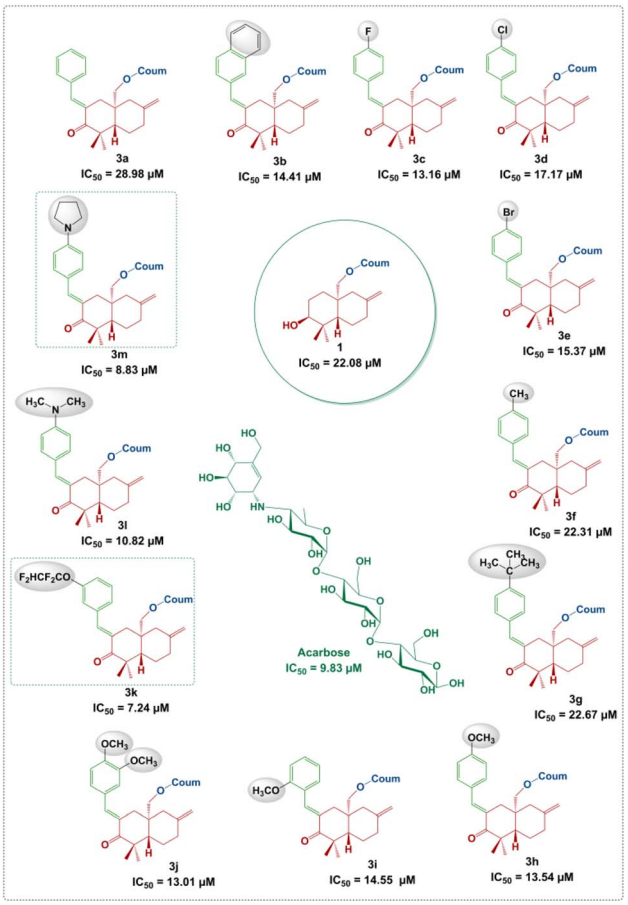

Fig. 6 α-Amylase inhibitory activity of the derivatives **3a–m** and acarbose.

substituted naphthalene system was found to be twice as active as compound **3a**, with an IC_{50} value of 14.41 ± 0.30 μM. The increase in the inhibitory activity of compound **3b** (R = naphthalene) compared to **3a** (R = Ph) may be due to the extent of conjugation in the two aromatic rings of naphthalene (Fig. 5). These results are in good agreement with those reported in the literature, showing that the presence of the naphthalene ring in the structure can contribute to inhibit the α-amylase enzyme.[26] Moreover, the alkyl group at the *p*-position of the phenyl group introduced by the aryl aldehyde in **3f** (R = *p*-$CH_3C_6H_4$) and **3g** (R = *p*-*tert*-BuC_6H_4) allowed to reach a moderate activity with IC_{50} values of 22.31 ± 0.90 and 22.67 ± 0.86 μM, respectively compared to **3a** (R = Ph). This finding allows noticing that the alkyl groups with a donor inductive (+I) effect did not improve significantly the anti-α-amylase activity.

Furthermore, the incorporation of a halogen atom at the *p*-position of the phenyl group from the arylidene system in **3c** (R = *p*-FC_6H_4), **3d** (R = *p*-ClC_6H_4) and **3e** (R = *p*-BrC_6H_4) enhances the inhibitory activity compared to **3a** (R=C_6H_5). Among the above-mentioned halogenated derivatives, the fluorinated one **3c** was found to exhibit the highest activity (IC_{50} = 13.16 ± 0.73 μM) (Fig. 6). This finding is consistent with the literature, showing that the incorporation of halogen atoms (F, Cl and Br) into the structure had an effect on the inhibition of α-amylase.[27,28] However, the double-methoxylated compound **3j** (*R* = 3,4-$(OCH_3)_2C_6H_3$) showed a slightly higher activity (IC_{50} = 13.01 ± 0.96 μM), than that of the mono-methoxylated compounds, **3h** (*p*-$OCH_3C_6H_4$; IC_{50} = 13.54 ± 0.54 μM) and **3i** (*o*-$OCH_3C_6H_4$; IC_{50} = 14.55 ± 0.30 μM). This finding shows that the more methoxyl groups there are, the more the activity increases even slightly. The electronic effects of methoxy groups (−I and +M) comparable to those of halogens (F, Cl and Br) may explain their significant activity.

Interestingly, compound **3k** (R = *m*-$OCF_2CHF_2C_6H_4$; IC_{50} = 7.24 ± 0.36 μM) displays more interesting activity than acarbose (IC_{50} = 9.83 ± 0.21 μM) and methoxylated derivatives **3h**, **3i** and **3j**. This result showed the net contribution of the introduced tetrafluoroethoxy fragment (–OCF_2CHF_2) to enhance the inhibition activity of the α-amylase enzyme (Fig. 6). It should also be mentioned that compound **3m** (IC_{50} = 8.83 ± 0.22 μM) bearing an aryl *p*-pyrrolidine moiety shows a higher activity than the standard compound (acarbose). This could be due, in part, to the donor (+M) mesomer effect of the nitrogen atom. The results indicated clearly that the α-amylase enzyme is more sensitive towards the *p*-pyrrolidine aryl moiety in **3m** compared to the acyclic amine in **3l** (IC_{50} = 10.82 ± 0.60 μM).

The inhibition potency of our arylidenes may be compared favorably with those of other arylidene compounds investigated by other research teams such as arylidene-linked chromane-2,4-dione analogs (7.7 ± 0.1 μM < IC_{50} < 60.7 ± 0.1 μM)[29] and 4-(arylidene)amino-1,2,4-traizole-5-thiol (IC_{50} = 1.65 ± 0.05–5.78 ± 0.18 μM).[30]

2.4. Kinetic studies

Kinetic studies on the parent molecule **1** and all synthesized compounds (**3a–m**) were performed to explain the mechanism of inhibition. The mechanism of enzyme inhibition was determined by graph fitting analysis using the Sigma-Plot enzyme kinetic software and kinetic parameters (V_{max} and K_M).

In particular, Fig. 7 shows the inhibition kinetic behavior of coladonin (**1**) and the most active arylidene derivatives ($IC_{50} \leq$ 10 μM), **3k**, **3l** and **3m**. As can be seen, the plots gave straight

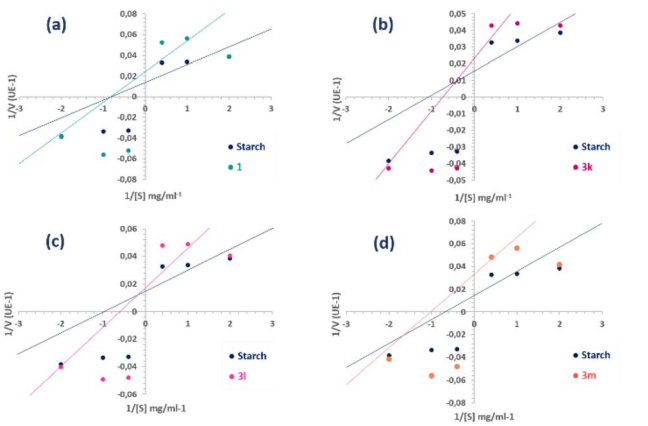

Fig. 7 Lineweaver–Burk plots of α-amylase inhibition at different starch (substrate) concentrations [S] in the presence and absence of compounds **1** (a), **3k** (b), **3l** (c) and **3m** (d).

lines with different slopes intersecting one another in different quadrants, showing a mixed-type inhibition. The difference found for these three compounds is that **3k** and **3l** are mixed competitive-non-competitive inhibitors, while **3m** is a mixed non-competitive-uncompetitive inhibitor. Analyzing the arrangement of these three compounds, the only difference observed was in the substituent at the *p*-position of the benzene ring of the arylidene. Specifically, compound **3k** features a *m*-tetrafluoroethoxyl group, **3l** possesses a *p*-*N*,*N*-dimethylamino group, while **3m** possesses a *p*-pyrrolidinyl group. Similarly, with the exception of **3j**, which exhibited non-competitive inhibition, all other arylidene derivatives proved to be mixed competitive-noncompetitive inhibitors.

Thus, in comparison with the plots of the semi-synthetic compounds and coladonin (**1**), we can deduce that the mechanism of inhibition has shifted from non-competitive to various mixed types of inhibition (Fig. 7). The identification of various inhibitor types has the potential to enhance research on α-amylase inhibitors.

Using the Dixon plot (Table S5†), the inhibitory constants (K_i) were determined for the most potent compounds. Compound **3k** showed a K_i value of 1.02 μM, indicating the most potent inhibitory activity.

2.5. Molecular docking analysis

Enzyme inhibitors are bioactive molecules capable of inhibiting or limiting the natural functioning of target enzymes by occupying their active pocket and competing with the substrate,[28,31] or by occupying distant allosteric sites. Indeed, the binding energy reflects the stability of the molecule-enzyme complex.[31,32]

Chemical compound-based virtual inspection is an effective process for confirming certain enzyme inhibitory activities and predicting molecular interactions.[31] Therefore, docking analyses were performed to reveal the mode of molecule-enzyme binding and to better understand the action manner of the novel synthesized compounds in the binding pocket or in other sites of the *Aspergillus oryzae* α-amylase enzyme using the AutoDock Vina software. In the present study, in addition to "active site docking", the "blind docking" approach was employed to investigate the possible binding sites of our compounds, distinct from the known binding site, due to their mixed inhibition characteristics against the α-amylase protein. In mixed-type inhibition, the inhibitor can bind to the enzyme whether or not the substrate is already bound.[33,34]

The binding positions of acarbose (the used standard reference) and the all compounds (in particular **3k**, **3l** and **3m**) in the structure of the α-amylase enzyme are shown in Fig. 8. The 2D-presentation of binding modes of compounds **3k**, **3l** and **3m**, compared to that of acarbose, is shown in Fig. 9.

Details of interactions and the binding energies of the selected compounds with the distant allosteric site and the active site residues are listed in Tables 1 and 2, respectively.

According to the docking results, all the selected compounds manifest an allosteric site docking, demonstrating a noncompetitive inhibition, which coincided with the results of noncompetitive inhibition for compounds **1** and **3j**, mixed non-competitive-uncompetitive inhibition for **3m** and mixed competitive-non-competitive inhibition for all remaining compounds.

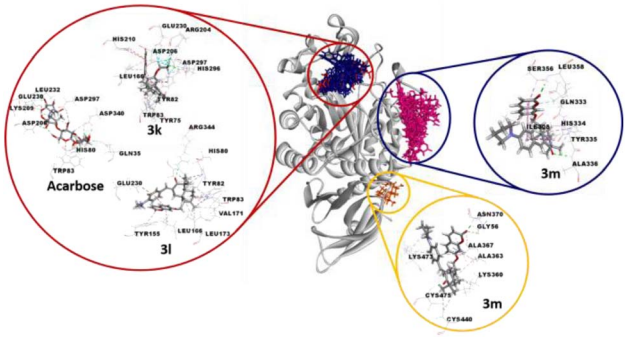

Fig. 8 Docking sites and 3D representations of the docked poses of the standard inhibitor (acarbose) and the three most active compounds **3k**, **3l** and **3m** into the α-amylase enzyme. Compounds **3a**, **3b**, **3c**, **3d**, **3e**, **3f**, **3g**, **3h**, **3i**, **3l**, **3k**, **3l** (blue molecules) and acarbose (red molecule) were docked into the active pocket (red circle), while compounds **1** and **3a–m** (pink molecules) were docked into an allosteric site (blue circle). In the yellow circle, compound **3m** was docked in a second allosteric site. The α-amylase enzyme is represented as a grey ribbon.

The compound **3m**, among the compounds with the best activity results, showed an excellent affinity (−8.4 kcal mol^{-1}) with the α-amylase enzyme. The pyrrolidinyl moiety formed alkyl interaction with ILE:308 and a π-donor hydrogen bond with the HIS:334 residue. The sesquiterpene system fits by a conventional hydrogen bond with the ALA:336 amino acid and a π-alkyl and π-sigma interactions with TYR:335. The coumarin moiety is involved in a conventional hydrogen bond with the LEU:358 amino acid, and a π-sigma interaction with the SER:356 residue (Fig. 9D). Overall, the blind docking results revealed that most derivatives, in the "non-active site", commonly adopt conventional hydrogen interactions with the residue ALA:336. In the case of the most active derivatives **3k**, **3l** and **3m** in the series, they adopt similar interactions and have residues in common with which they react, such as ILE:308, HIS 334, TYR:335, and ALA:336 (hydrogen bonds in all 3 cases).

It is worth noting that, in the blind docking process, compound **3m** demonstrated a remarkable affinity for a second allosteric site, exhibiting a binding energy value of −8.0 kcal-mol^{-1}. This affinity was established through the formation of 14 interactions (2 conventional hydrogen bonds, 1 carbon hydrogen bond, 5 π-alkyl and 6 alkyl bonds) with eight different amino acids (GLY:56, LYS:360, ALA:363, ALA:367, ASN:370, CYS:440, LYS:473 and CYS:475). This observation can be attributed to its partial uncompetitive inhibition mode (Fig. 9E).

However, many considerable results of the selected molecules docked in the active site of the α-amylase enzyme were observed. Based on the binding energies (−8.2 to −10.2 kcal mol^{-1}), all compounds (except **1**, **3j** and **3m**) proved to have high affinity within the active cavity of the α-amylase enzyme, since they exhibit mixed competitive–non-competitive

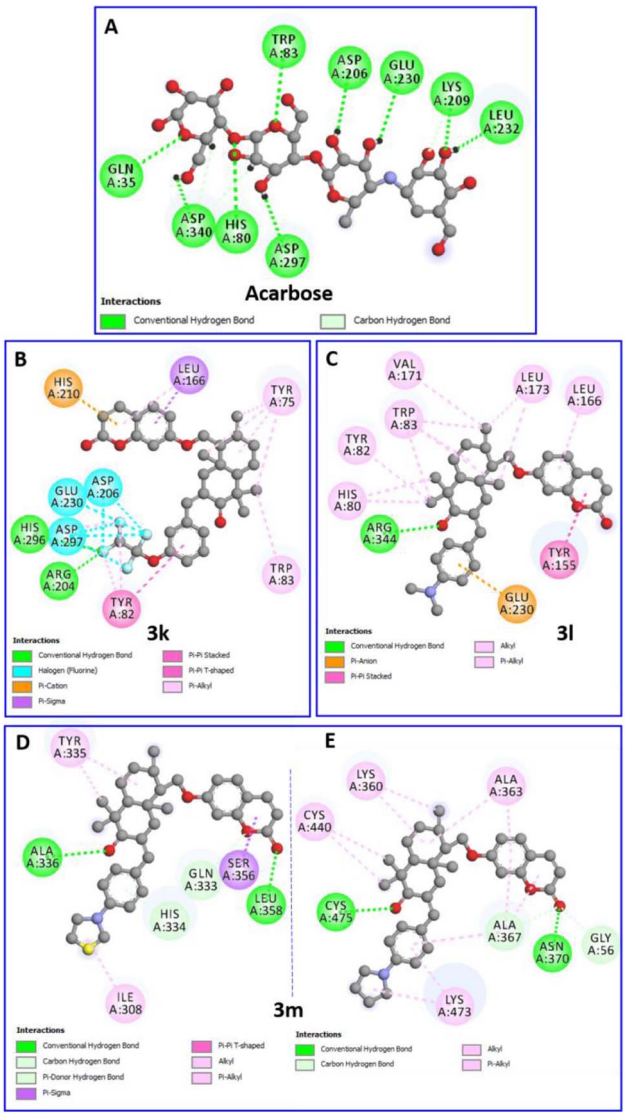

Fig. 9 Two-dimensional profiles showing the interaction modes of acarbose (A) and the three most active compounds **3k** (B), **3l** (C) and **3m** (D and E) into the binding pocket or/and allosteric site of the α-amylase enzyme (PDB: 7TAA).

inhibition. Interestingly and as expected, all these compounds are perfectly localized in the active pocket of the target enzyme.

Acarbose (−7.9 kcal mol^{-1}) forms nine hydrogen bonds with nine different residues (Table 1), including the two key amino acids essential for the cleavage of glycosidic bindings, namely, the nucleophilic residue ASP:206 as well as the catalytic acid/base residue GLU:230.[31] Therefore, the compound ability to fit with these key residues increases the potency to inhibit polysaccharide hydrolysis.

Interestingly, the complex of the **3k** derivative with the target enzyme showed exceptional stability (−10.2 kcal mol^{-1}) superior to that of acarbose. In the binding profile of the compound **3k**, the 1,1,2,2-tetrafluoroethoxyl group alone is implicated in fifteen interactions with six amino acids. It formed three hydrogen bonds with ARG:204 and HIS:296, eight halogen (Fluorine) bonds with ASP:206, GLU:230 and ASP:297, and four π-alkyl bonds with TYR:82 and HIS:296. The aromatic ring of the arylidene group fits with a π–π stacked binding with TYR:82. The sesquiterpene moiety performed five π-alkyl bonds with TYR:75 and TRP:83. However, the coumarin moiety forms a π–π T-shaped and a π-cation bond with HIS:210 and two π-alkyl interactions with LEU:166 (Fig. 9B).

Furthermore, the binding profile of the compound **3l**, exhibiting an impressive binding energy (−8.9 kcal mol^{-1}), indicates that it is engaged in fourteen non-covalent interactions with nine residues. The arylidene group fits by a π-anion bond with the key residue GLU:230. The carbonyl in C-3′ forms a conventional hydrogen bond with ARG:344. The rest of the sesquiterpene moiety performed seven π-alkyl interactions with HIS:80, TYR:82 and TRP:83 residues and three alkyl bonds with VAL:171 and LEU:173. A π–π stacked binding with TYR:155 and a π-alkyl bond with LEU:166 were formed by the coumarin fragment (Fig. 9C).

2.6. Toxicity analysis

It is crucial to evaluate the toxicity of the synthesized chemical compounds with medical significance. An *in silico* approach (**https://www.organic-chemistry.org/prog/peo/**) is indeed available for predicting specific toxicity risks such as mutagenicity, tumorigenicity, irritation and reproductive effects. All the predicted compounds were found to be free from irritation risk. Moreover, the majority of compounds, except **3l** and **3m**, exhibited no mutagenicity or tumorigenicity risks. Similarly, concerning the reproductive effects, only **3h** and **3j** presented toxicity risks, while the remaining compounds were deemed safe (Table S4†). The observed toxicity might be attributed to the presence of oxygen or nitrogen, particularly in the para position of the arylidene aromatic ring.

3 Experimental

3.1. General procedures

All chemicals were obtained from commercial suppliers and used without further purification. ^{1}H (600 MHz) and ^{13}C (deduced from HSQC and HMBC spectra) NMR spectra were recorded using a Bruker AVANCE III, with $CDCl_3$ as the solvent and TMS as the internal standard. Melting points were measured using a Buchi melting point apparatus, model B-545. ESI-HRMS spectra were recorded with a platform consisting of an HTC PAL® 4 autosampler (CTC Analytics AG, Zwingen, Switzerland), an Accela U-HPLC system with quaternary pumps, and an Exactive Orbitrap mass spectrometer equipped with a heated electrospray ionization (H-ESI) probe (both from Thermo Fisher Scientific, Bremen, Germany). α-Amylase was extracted from porcine pancreas (Sigma Aldrich 6255, 1151 Umg^{-1} of protein, Sigma Aldrich, Saint Louis, MO).

3.2. Plant material

The roots of *F. tunetana* were collected from the region of Menzel Kamel (Tunisia) (35°38′21.4″N 10°36′31.2″E), in April

Table 1 α-Amylase inhibition (IC_{50} ± SD μM), binding energy (kcal mol^{-1}) and interaction details of compounds **1** and **3a–m** into the allosteric site of the α-amylase enzyme (PDB: 7TAA)[a,c]

N°	α-Amylase inhibition	Binding energy	Interaction detail: NI/NIAA: IAA
1	22.08 ± 1.10	−7.1	9/6: THR:32[b], ALA:33[b], TYR:335, ALA:336, ALA:342, LEU:349
3a	28.98 ± 0.65	−7.5	8/5: TYR:335[b], ALA:336[b], ALA:342, GLU:345, LEU:349
3b	14.41 ± 0.30	−8.6	10/7: TYR:335, ALA:336[b], GLY:337, ALA:342, GLU:345, LEU:349, SER:350
3c	13.16 ± 0.73	−8.0	9/6: CYS:30, TYR:335[b], ALA:336[b], ALA:342, GLU:345, LEU:349
3d	17.17 ± 0.50	−7.4	7/5: HIS:334, TYR:335, ALA:336, GLU:345, LEU:349
3e	15.37 ± 0.29	−7.6	9/5: ASN:31, THR:32[b], TYR:335, ALA:336, LEU:349
3f	22.31 ± 0.90	−8.1	5/3: TYR:335, ALA:336[b], LEU:349
3g	22.67 ± 0.86	−7.9	8/5: HIS:334, TYR:335, ALA:336[b], GLU:345, LEU:349
3h	13.54 ± 0.54	−8.0	6/5: ASN:306, TYR:335, ALA:336[b], GLU:357[b], LEU:358[b]
3i	14.55 ± 0.30	−7.6	6/5: THR:32[b], TYR:335, ALA:336, GLU:345, LEU:349
3j	13.01 ± 0.96	−8.0	10/7: THR:32[b], HIS:334, TYR:335, ALA:336[b], GLY:338[b], ALA:342, LEU:349
3k	7.24 ± 0.36	−8.3	9/8: ILE:308, GLN:333, HIS:334[b], TYR:335, ALA:336[b], LEU:349, SER:350, GLU:357[b]
3l	10.82 ± 0.60	−9.4	8/5: TYR:335, ALA:336[b], ALA:342, GLU:345[b], LEU:349
3m	8.83 ± 0.22	−8.4	7/6: ILE:308, HIS:334, TYR:335, ALA:336[b], SER:356, LEU:358[b]

[a] NI: Number of interactions, NIAA: number of interacting amino acids, IAA: interacting amino acids. [b] 1 Hydrogen bond. [c] α-Amylase inhibitory activity as IC_{50} ± SD (μM) is the compound concentration providing 50% of inhibition. IC_{50} values followed by the same letter are not significantly different at *p*-value less than 0.05. The binding energy is in kcal mol^{-1}.

Table 2 Interaction details of the selected compounds and acarbose into the active pocket of the α-amylase enzyme (PDB: 7TAA)[a,e]

N°	Binding energy	Interaction detail: NI/NIAA: IAA
3a	−8.8	14/8: HIS:80, TYR:82, HIS:122, TYR:155, **ASP:206**, HIS:210[b], LEU:232, ARG:344[d]
3b	−9.6	13/10: HIS:80, TYR:82, TYR:155, LEU:166, ARG:204[c], **ASP:206**, HIS:210, LEU:232, HIS:296[b], ASP:297
3c	−9.6	11/8: TYR:75, TYR:82, TRP:83[b], TYR:155[b], LEU:166, **ASP:206**, **GLU:230**, ARG:344[b]
3d	−10.1	10/7: TYR:75, HIS:80, TYR:82, TRP:83, LEU:166, **GLU:230**, HIS:296[b]
3e	−10.0	10/7: TYR:75, HIS:80, TYR:82, TRP:83, LEU:166, **GLU:230**, HIS:296[b]
3f	−8.7	15/10: HIS:80, TYR:82, TRP:83, TYR:155, LEU:166, LEU:173, HIS:210, **GLU:230**, LEU:232, ARG:344[b]
3g	−8.2	14/13: TYR:75, HIS:80, TYR:82, TRP:83, ILE:152[b], GLY:167[b], ASP:168, LEU:173, HIS:210, **GLU:230**, LEU:232, ASP:297, ARG:344[b]
3h	−8.5	14/11: HIS:80, TYR:82, TRP:83, ILE:152[b], TYR:155, LEU:166, GLY:167[b], LEU:173, HIS:210[b], **GLU:230**, ARG:344[b]
3i	−9.1	15/10: HIS:80, HIS:122, TYR:155, LEU:166, LEU:173, **ASP:206**, HIS:210[b], LEU:232, ASP:340, ARG:344[c]
3k	−10.2	25/10: TYR:75, TYR:82, TRP:83, LEU:166, ARG:204[c], **ASP:206**, HIS:210, **GLU:230**, HIS:296[b], ASP:297
3l	−8.9	14/9: HIS:80, TYR:82, TRP:83, TYR:155, LEU:166, VAL:171, LEU:173, **GLU:230**, ARG:344[b]
Acr	−7.9	11/9: GLN:35[b], HIS:80[b], TRP:83[b], **ASP:206**[b], LYS:209[b], **GLU:230**[b], LEU:232[b], ASP:297[b], ASP:340[b]

[a] Acr: acarbose (the used standard reference), NI: number of interactions, NIAA: number of interacting amino acids, IAA: interacting amino acids. [b] 1 Hydrogen bond. [c] 2 Hydrogen bonds. [d] 3 Hydrogen bonds, bold type indicates interactions with key amino acids. [e] The binding energy is in Kcal mol^{-1}.

2019. The botanical identification was carried out by distinguished professor Fethia Harzallah-Skhiri, and a voucher specimen (FT/19) was deposited in the laboratory mentioned above.

3.3. Extraction and isolation

First, 5 kg of fresh roots of the *F. tunetana* plant were macerated at room temperature in a MeOH/water mixture (7 : 3/v : v) for 7 days. The aqueous phase, after evaporation of methanol, was extracted with chloroform ($CHCl_3$). The $CHCl_3$ extract (15 g), namely RC, was separated using a silica gel chromatographic column, eluted initially with a petroleum ether/EtOAc mixture of increasing polarity (20 to 100% EtOAc), and then by adding MeOH to EtOAc (0 to 100% MeOH) in 15 fractions (RC_1–RC_{15} (g): 0.66; 0.79; 0.61; 0.28; 1.5; 0.18; 0.80; 0.32; 0.21; 0.25; 2.80; 1.31; 0.75; 0.35; and 2.4), according to TLC analysis and sulfur vanillin revelation. Coladonin **1** (1.5 g) was isolated from the RC_{11} fraction following precipitation in *n*-hexane.

3.3.1 Coladonin (1). White powder. NMR ^1H ($CDCl_3$, 600 MHz) δ_H: 7.64 (1H, d, J = 9.4 Hz, H-4), 7.36 (1H, d, J = 8.5 Hz, H-5), 6.83 (1H, m, H-6), 6.82 (1H, m, H-8), 6.25 (1H, d, J = 9.5 Hz, H-3), 4.93 (1H, s, H-12′a), 4.55 (1H, s, H-12′b), 4.21 (1H, dd, J = 9.7; 4.2 Hz, H-11′a), 4.18 (1H, dd, J = 9.6; 7.8 Hz, H-11′b), 3.31 (1H, dd, J = 11.7; 4.2 Hz, H-3′), 2.47 (1H, ddd, J = 13.2; 4.2; 2.5 Hz, H-7′a), 2.10 (1H, td, J = 13.2; 5.0 Hz, H-7′b), 2.21 (1H, dd, J = 6.6; 4.6 Hz, H-9′), 1.82 (1H, dt, J = 13.2; 3.5 Hz, H-1′a), 1.78 (1H, m, H-6′a), 1.75 (1H, dq, J = 13.1; 4.0 Hz, H-2′a), 1.63 (1H, m, H-2′b), 1.47 (1H, m, H-1′b), 1.46 (1H, m, H-6′b), 1.18 (1H, dd, J = 12.5; 2.7 Hz, H-5′), 1.03 (3H, s, H-13′), 0.85 (3H, s, H-15′), 0.82 (3H, s, H-14′). NMR ^{13}C ($CDCl_3$, 150 MHz) δ_C:162.4 (C-7), 161.6 (C-2), 156.1 (C-9), 146,5 (C-8′), 143.8 (C-4), 129.0 (C-5), 113.3 (C-3), 113.4 (C-6), 112.6 (C-10), 108.1 (C-12′), 101.6 (C-8), 78.8 (C-3′), 65.3 (C-11′), 54.9 (C-9′), 54.4 (C-5′), 39.1 (C-4′), 38.9 (C-10′), 37.4 (C-1′), 37.2 (C-7′), 27.7 (C-2′), 28.4 (C-13′), 23.5 (C-6′), 15.6 (C-14′), 15.6 (C-15′).

3.4. General procedure for oxidation at C-3′–OH

Coladonin **1** (1 g, 2.6 mmol) was dissolved in acetone and 5 drops of the prepared Jones reagent were added to the reaction flask placed in an ice bath, and then the mixture was stirred for 3 h.[35] After evaporation of acetone, 100 mL of cold water was added and the mixture was extracted with ethyl acetate (3 × 25 mL), and the organic phase was filtered and dried with Na_2SO_4. Finally, a white solid **2** (0.92 g, 92%) was obtained by column chromatography (petroleum ether/EtOAc: (80 : 20)).

3.4.1 7-(((1R,4aS,8aR)-5,5,8a-trimethyl-2-methylene-6-oxodecahydronaphthalen-1-yl)methoxy)-2*H*-chromen-2-one (2). White powder, yield: 92%; m.p.: 175 °C. NMR ^{1}H ($CDCl_3$, 600 MHz) δ_H: 7.64 (1H, d, J = 9.5 Hz, H-4), 7.37 (1H, d, J = 9.3 Hz, H-5), 6.83 (1H, dd, J = 7.0; 2.3 Hz, H-6), 6.82 (1H, d, J = 2.2 Hz, H-8), 6.26 (1H, d, J = 9.5 Hz, H-3), 4.98 (1H, s, H-12′a), 4.60 (1H, s, H-12′b), 4.24 (1H, dd, J = 8.2; 5.5 Hz, H-11′a), 4.22 (1H, dd, J = 8.3; 3.4 Hz, H-11′b), 2.69 (1H, ddd, J = 15.3; 13.3; 6.2 Hz, H-2′a), 2.51 (1H, ddd, J = 13.1; 4.0; 2.5 Hz, H-7′a), 2.41 (1H, ddd, J = 15.3; 5.2; 3.5 Hz, H-2′b), 2.30 (1H, t, J = 5.5 Hz, H-9′), 2.15 (1H, m, H-7′b), 2.10 (1H, ddd, J = 13.3; 6.2; 3.5 Hz, H-1′a), 1.81 (1H, td, J = 13.3; 5.3 Hz, H-1′b), 1.73 (1H, m, H-6′a), 1.58 (1H, m, H-6′b), 1.67 (1H, dd, J = 12.4; 2.6 Hz, H-5′), 1.13 (3H, s, H-13′), 1.07 (3H, s, H-14′), 1.04 (3H, s, H-15′). NMR ^{13}C ($CDCl_3$, 150 MHz) δ_C:215.9 (C-3′), 162.2 (C-7), 161.4 (C-2), 156.1(C-9), 145.8 (C-8′), 143.7 (C-4), 129.1 (C-5), 113.4 (C-3), 113.3 (C-6), 112.8 (C-10), 108.9 (C-12′), 101.5 (C-8), 65.9 (C-11′), 55.2 (C-5′), 54.3 (C-9′), 48.1 (C-4′), 38.8 (C-10′), 37.6 (C-1′), 37.2 (C-7′), 34.7 (C-2′), 25.8 (C-13′), 24.6 (C-6′), 22.0 (C-14′), 14.9 (C-15′).ESI-HRMS $[M + H]^+$ calcd. for $[C_{24}H_{29}O_4]^+$: 381.20658, found: 381.20663.

3.5. General procedure for the preparation of analogues (3a–m)

A solution of **2** (50 mg, 0.13 mmol) and KOH (1.5 equiv.) in ethanol, aryl-aldehyde (1.5 equiv.) was added, and the mixture was reacted for 24 h.[30] The crude was diluted in distilled water, neutralized with H_2SO_4 solution (2 M) and extracted with EtOAc (3 × 10 mL). After the removal of EtOAc, the resulting mixture was purified by silica gel column chromatography (petroleum ether/EtOAc: (80 : 20)) to give the derivatives **3a–m**.

3.5.1 7-(((1R,4aS,8aR)-7-((*E*)-benzylidene)-5,5,8a-trimethyl-2-methylene-6-oxodecahydronaphthalen-1-yl)methoxy)-2*H*-chromen-2-one (3a). Yellow powder, yield: 86%; m.p.: 80 °C. NMR ^{1}H ($CDCl_3$, 600 MHz) δ_H: 7.66 (1H, d, J = 9.5 Hz, H-4), 7.57 (1H, d, J = 2.1 Hz, H-7″), 7,46 (2H, d, J = 2.1 Hz, H-2″,6″), 7.40 (1H, d, J = 8.6 Hz, H-5), 7.37 (2H, t, J = 7.5 Hz, H-3″,5″), 7.31 (1H, m, H-4″), 6.86 (1H, dd, J = 8.5; 2.4 Hz, H-6), 6.85 (1H, d, J = 2.4 Hz, H-8), 6.27 (1H, d, J = 9.5 Hz, H-3), 4.98 (1H, s, H-12′a), 4.55 (1H, s, H-12′b), 4.25 (1H, dd, J = 9.9; 6.0 Hz, H-11′a), 4.22 (1H, dd, J = 9.9; 5.7 Hz, H-11′b), 3.24 (1H, dd, J = 16.4; 1.1 Hz, H-1′a), 2.74 (1H, dd, J = 16.3; 2.8 Hz, H-1′b), 2.51 (1H, ddd, J = 12.9; 4.1; 2.7 Hz, H-7′a), 2.48 (1H, m, H-9′), 2.16 (1H, td, J = 12.9; 4.1 Hz, H-7′b), 1.92 (1H, dd, J = 12.7; 3.5 Hz, H-5′), 1.80 (1H, dq, J = 13.0; 3.0 Hz, H-6′a), 1.52 (1H, qd, J = 13.2; 4.2 Hz, H-6′b), 1.21 (3H, s, H-13′), 1.18 (3H, s, H-14′), 0.78 (3H, s, H-15′). NMR ^{13}C ($CDCl_3$, 150 MHz) δ_C:207.0 (C-3′), 162.1 (C-7), 161.4 (C-2), 156.1(C-9), 146.1 (C-8′), 143.7 (C-4), 137.9 (C-7″), 135.8 (C-1″), 133.0 (C-2′), 130.6 (C-2″,6″), 129.0 (C-5), 128.8 (C-3″,5″), 128.6 (C-4″), 113.5 (C-3), 113.0 (C-6), 112.8 (C-10), 108.0 (C-12′), 101.7 (C-8), 66.3 (C-11′), 52.9 (C-5′), 52.8 (C-9′), 45.7 (C-4′), 41.9 (C-1′), 39.0 (C-10′), 37.5 (C-7′), 30.0 (C-13′), 26.3 (C-6′), 23.0 (C-14′), 14.0 (C-15′). ESI-HRMS $[M + H]^+$ calcd. for $[C_{31}H_{33}O_4]^+$: 469.23788, found: 469.23822.

3.5.2 7-(((1R,4aS,8aR,E)-5,5,8a-trimethyl-2-methylene-7-(naphthalen-2-ylmethylene)-6-oxodecahydronaphthalen-1-yl)methoxy)-2*H*-chromen-2-one (3b). Yellow powder, yield: 82%; m.p.: 115 °C. NMR ^{1}H ($CDCl_3$, 600 MHz) δ_H: 7.88 (1H, s, H-6″), 7.81 (2H, d, J = 8.4 Hz, H-3″,8″), 7.76 (1H, d, J = 8.1 Hz, H-11″), 7.75 (1H, d, J = 2.6 Hz, H-7″), 7.63 (1H, d, J = 9.5 Hz, H-4), 7.55 (1H, dd, J = 8.6, 1.6 Hz, H-2″), 7.49 (1H, m, H-9″), 7.45 (1H, m, H-10″), 7.30 (1H, d, J = 8.6 Hz, H-5), 6.82 (1H, d, J = 2.4 Hz, H-8), 6.79 (1H, dd, J = 8.5; 2.4 Hz, H-6), 6.27 (1H, d, J = 9.5 Hz, H-3), 4.98 (1H, s, H-12′a), 4.55 (1H, s, H-12′b), 4.24 (1H, dd, J = 9.9; 6.0 Hz, H-11′a), 4.21 (1H, dd, J = 9.9; 5.6 Hz, H-11′b), 3.34 (1H, dd, J = 16.2; 0.8 Hz, H-1′a), 2.82 (1H, dd, J = 16.2; 2.8 Hz, H-1′b), 2.52 (1H, dt, J = 10.7; 5.0 Hz, H-7′a), 2.50 (1H, t, J = 5.3 Hz, H-9′), 2.17 (1H, td, J = 12.9; 4.0 Hz, H-7′b), 1.96 (1H, dd, J = 12.7; 3.5 Hz, H-5′), 1.82 (1H, dq, J = 13.1; 4.1 Hz, H-6′a), 1.54 (1H, qd, J = 13.1; 4.2 Hz H-6′b), 1.24 (3H, s, H-13′), 1.20 (3H, s, H-14′), 0.80 (3H, s, H-15′). NMR ^{13}C ($CDCl_3$, 150 MHz) δ_C:206.9 (C-3′), 162.0 (C-7), 161.3 (C-2), 156.1 (C-9), 146.2 (C-8′), 143.7 (C-4), 138.1 (C-7″), 135.8 (C-1″), 133.3 (C-2′), 133.2 (C-9″), 130.6 (C-10″), 129.0 (C-5), 128.7 (C-5″), 128.2 (C-3″), 128.2 (C-8″), 128.6 (C-4″), 127.5 (C-2″), 127.2 (C-7″), 127.0 (C-6″), 113.5 (C-3), 113.0 (C-6), 112.8 (C-10), 108.5 (C-12′), 101.8 (C-8), 66.4 (C-11′), 53.1 (C-5′), 53.0 (C-9′), 45.7 (C-4′), 42.0 (C-1′), 39.1 (C-10′), 37.6 (C-7′), 30.0 (C-13′), 26.4 (C-6′), 23.1 (C-14′), 14.1 (C-15′). ESI-HRMS $[M + H]^+$ calcd. for $[C_{35}H_{35}O_4]^+$: 519.25353, found: 519.25397.

3.5.3 7-(((1R,4aS,8aR)-7-((*E*)-4-fluorobenzylidene)-5,5,8a-trimethyl-2-methylene-6-oxodecahydronaphthalen-1-yl)methoxy)-2*H*-chromen-2-one (3c). Yellow powder, yield: 75%; m.p.: 120 °C. NMR ^{1}H ($CDCl_3$, 600 MHz) δ_H: 7.67 (1H, d, J = 9.5 Hz, H-4), 7.53 (1H, d, J = 2.0 Hz, H-7″), 7.42 (2H, dd, J = 9.1; 5.0 Hz, H-2″,6″), 7.42 (1H, d, J = 8.5 Hz, H-5), 7.03 (2H, t, J = 8.6 Hz, H-3″,5″), 6.85 (1H, dd, J = 8.4; 2.5 Hz, H-6), 6.84 (1H, d, J = 2.3 Hz, H-8), 6.28 (1H, d, J = 9.5 Hz, H-3), 4.98 (1H, s, H-12′a), 4.56 (1H, s, H-12′b), 4.25 (1H, dd, J = 9.9; 5.8 Hz, H-11′a), 4.23 (1H, dd, J = 9.9; 5.7 Hz, H-11′b), 3.17 (1H, d, J = 16.3 Hz, H-1′a), 2.71 (1H, dd, J = 16.3; 2.7 Hz, H-1′b), 2.51 (1H, ddd, J = 13.0; 4.1; 2.9 Hz, H-7′a), 2.49 (1H, t, J = 6.6 Hz, H-9′), 2.16 (1H, td, J = 13.0; 4.2 Hz, H-7′b), 1.92 (1H, dd, J = 12.7; 3.5 Hz, H-5′), 1.80 (1H, dq, J = 13.0; 4.0 Hz, H-6′a), 1.52 (1H, qd, J = 13.2; 4.2 Hz, H-6′b), 1.20 (3H, s, H-13′), 1.17 (3H, s, H-14′), 0.78 (3H, s, H-15′). NMR ^{13}C ($CDCl_3$, 150 MHz) δ_C:206.9 (C-3′), 162.0 (C-4″), 161.9 (C-7), 161.3 (C-2), 156.1(C-9), 146.2 (C-8′), 143.6 (C-4), 136.9 (C-7″), 132.4 (C-2′), 132.5 (C-2″,6″), 131.9 (C-1″), 129.1 (C-5), 115.9 (C-3″,5″), 113.6 (C-3), 113.1 (C-6), 112.8 (C-10), 108.4 (C-12′), 101.6 (C-8), 66.4 (C-11′), 52.9 (C-5′), 52.8 (C-9′), 45.4 (C-4′), 41.9 (C-1′), 40.0 (C-10′), 37.5 (C-7′), 30.0 (C-13′), 26.3 (C-6′), 23.0 (C-14′), 14.0 (C-15′). ESI-HRMS $[M + H]^+$ calcd. for $[C_{31}H_{32}FO_4]^+$: 487.22846, found: 487.22888.

3.5.4 7-(((1R,4aS,8aR)-7-((*E*)-4-chlorobenzylidene)-5,5,8a-trimethyl-2-methylene-6-oxodecahydronaphthalen-1-yl)

methoxy)-2*H*-chromen-2-one (3d). Yellow powder, yield: 90%; m.p.: 105 °C. NMR ^{1}H ($CDCl_3$, 600 MHz) δ_H: 7.67 (1H, d, J = 9.5 Hz, H-4), 7.51 (1H, d, J = 2.1 Hz, H-7″), 7.43 (1H, d, J = 9.2 Hz, H-5), 7.36 (2H, d, J = 8.5 Hz, H-2″,6″), 7.31 (2H, d, J = 8.5 Hz, H-3″,5″), 6.84 (1H, dd, J = 9.2; 2.4 Hz, H-6), 6.83 (1H, d, J = 2.3 Hz, H-8), 6.28 (1H, d, J = 9.5 Hz, H-3), 4.98 (1H, s, H-12′a), 4.55 (1H, s, H-12′b), 4.26 (1H, dd, J = 10.0; 5.7 Hz, H-11′a), 4.21 (1H, dd, J = 10.0; 5.8 Hz, H-11′b), 3.16 (1H, d, J = 16.3 Hz, H-1′a), 2.70 (1H, dd, J = 16.2; 2.9 Hz, H-1′b), 2.51 (1H, ddd, J = 12.8; 3.9; 2.8 Hz, H-7′a), 2.48 (1H, t, J = 5.5 Hz, H-9′), 2.16 (1H, td, J = 13.0; 4.2 Hz, H-7′b), 1.92 (1H, dd, J = 12.7; 3.5 Hz, H-5′), 1.80 (1H, dq, J = 12.9; 4.0 Hz, H-6′a), 1.52 (1H, qd, J = 13.2; 4.2 Hz, H-6′b), 1.20 (3H, s, H-13′), 1.17 (3H, s, H-14′), 0.77 (3H, s, H-15′). NMR ^{13}C ($CDCl_3$, 150 MHz) δ_C:206.6 (C-3′), 161.9 (C-7), 161.3 (C-2), 156.1(C-9), 146.1 (C-8′), 143.7 (C-4), 136.6 (C-7″), 134.8 (C-4″), 134.3 (C-1″), 133.6 (C-2′), 131.8 (C-2″,6″), 129.1 (C-5), 129.1 (C-3″,5″), 113.6 (C-3), 113.1 (C-6), 112.8 (C-10), 108.5 (C-12′), 101.6 (C-8), 66.4 (C-11′), 53.0 (C-5′), 52.8 (C-9′), 45.7 (C-4′), 41.9 (C-1′), 38.9 (C-10′), 37.5 (C-7′), 30.0 (C-13′), 26.3 (C-6′), 23.1 (C-14′), 14.0 (C-15′). ESI-HRMS $[M + H]^+$ calcd. for $[C_{31}H_{32}ClO_4]^+$: 503.19891, found: 503.19925.

3.5.5 7-(((1R,4aS,8aR)-7-((*E*)-4-bromobenzylidene)-5,5,8a-trimethyl-2-methylene-6-oxodecahydronaphthalen-1-yl) methoxy)-2*H*-chromen-2-one (3e). Yellow powder, yield: 93%; m.p.: 139 °C. NMR ^{1}H ($CDCl_3$, 600 MHz) δ_H: 7.67 (1H, d, J = 9.5 Hz, H-4), 7.48 (1H, d, J = 2.3 Hz, H-7″), 7.45 (1H, d, J = 8.5 Hz, H-3″,5″), 7.43 (1H, d, J = 9.2 Hz, H-5), 7.29 (2H, d, J = 8.5 Hz, H-2″,6″), 6.84 (1H, d, J = 2.7 Hz, H-8), 6.83 (1H, dd, J = 8.9; 2.4 Hz, H-6), 6.28 (1H, d, J = 9.5 Hz, H-3), 4.98 (1H, s, H-12′a), 4.56 (1H, s, H-12′b), 4.26 (1H, dd, J = 9.9; 5.7 Hz, H-11′a), 4.20 (1H, dd, J = 9.9; 5.8 Hz, H-11′b), 3.14 (1H, d, J = 16.3 Hz, H-1′a), 2.70 (1H, dd, J = 16.3; 2.8 Hz, H-1′b), 2.51 (1H, ddd, J = 12.9; 4.0; 2.9 Hz, H-7′a), 2.48 (1H, t, J = 5.8 Hz, H-9′), 2.16 (1H, td, J = 13.0; 4.1 Hz, H-7′b), 1.92 (1H, dd, J = 12.7; 3.5 Hz, H-5′), 1.80 (1H, dq, J = 13.0; 3.9 Hz, H-6′a), 1.53 (1H, qd, J = 13.1; 4.2 Hz, H-6′b), 1.20 (3H, s, H-13′), 1.17 (3H, s, H-14′), 0.77 (3H, s, H-15′). NMR ^{13}C ($CDCl_3$, 150 MHz) δ_C: 206.8 (C-3′), 161.9 (C-7), 161.3 (C-2), 156.1(C-9), 146.1 (C-8′), 143.7 (C-4), 136.6 (C-7″), 134.6 (C-1″), 133.7 (C-2′), 132.0 (C-2″,6″), 131.9 (C-3″,5″), 129.2 (C-5), 123.1 (C-4″), 113.6 (C-3), 113.1 (C-6), 112.9 (C-10), 108.5 (C-12′), 101.6 (C-8), 66.4 (C-11′), 52.9 (C-5′), 52.9 (C-9′), 45.7 (C-4′), 41.8 (C-1′), 38.9 (C-10′), 37.6 (C-7′), 30.1 (C-13′), 26.3 (C-6′), 23.4 (C-14′), 14.0 (C-15′). ESI-HRMS $[M + H]^+$ calcd. for $[C_{31}H_{32}BrO_4]^+$: 547.14840, found: 547.14874.

3.5.6 7-(((1R,4aS,8aR)-5,5,8a-trimethyl-7-((*E*)-4-methylbenzylidene)-2-methylene-6-oxodecahydronaphthalen-1-yl) methoxy)-2*H*-chromen-2-one (3f). Yellow powder, yield: 84%; m.p.: 93 °C. NMR ^{1}H ($CDCl_3$, 600 MHz) δ_H: 7.67 (1H, d, J = 9.5 Hz, H-4), 7.56 (1H, d, J = 1.9 Hz, H-7″), 7.42 (1H, d, J = 8.5 Hz, H5), 7.36 (2H, d, J = 8.1 Hz, H-2″,6″), 7.18 (1H, d, J = 8.0 Hz, H-3″,5″), 6.88 (1H, dd, J = 8.5; 2.4 Hz, H-6), 6.86 (1H, d, J = 2.3 Hz, H-8), 6.28 (1H, d, J = 9.5 Hz, H-3), 4.98 (1H, s, H-12′a), 4.55 (1H, s, H-12′b), 4.26 (1H, dd, J = 10.1; 6.3 Hz, H-11′a), 4.23 (1H, dd, J = 10.1; 5.8 Hz, H-11′b), 3.23 (1H, dd, J = 16.3; 0.8 Hz, H-1′a), 2.73 (1H, dd, J = 16.2; 2.7 Hz, H-1′b), 2.51 (1H, ddd, J = 12.8; 3.9; 2.9 Hz, H-7′a), 2.49 (1H, t, J = 5.6 Hz, H-9′), 2.18 (1H, td, J = 13.0; 4.1 Hz, H-7′b), 1.92 (1H, dd, J = 12.7; 3.5 Hz, H-5′), 1.80 (1H, dq, J = 12.8; 4.0 Hz, H-6′a), 1.52 (1H, qd, J = 13.2; 4.2 Hz, H-6′b), 1.20 (3H, s, H-13′), 1.17 (3H, s, H-14′), 0.76 (3H, s, H-15′). NMR ^{13}C ($CDCl_3$, 150 MHz) δ_C: 206.9 (C-3′), 162.1 (C-7), 161.3 (C-2), 156.1(C-9), 146.2 (C-8′), 143.7 (C-4), 139.1 (C-4″), 138.1 (C-7″), 132.9 (C-1″), 132.0 (C-2′), 130.8 (C-2″,6″), 129.6 (C-3″,5″), 129.2 (C-5), 113.5 (C-3), 113.0 (C-6), 112.8 (C-10), 108.4 (C-12′), 101.8 (C-8), 66.3 (C-11′), 52.8 (C-5′), 53.0 (C-9′), 45.6 (C-4′), 42.1 (C-1′), 38.9 (C-10′), 37.6 (C-7′), 30.1 (C-13′), 26.4 (C-6′), 23.0 (C-14′), 14.5 (C-15′). ESI-HRMS $[M + H]^+$ calcd. for $[C_{32}H_{35}O_4]^+$: 483.25353, found: 483.25345.

3.5.7 7-(((1R,4aS,8aR)-7-((*E*)-4-(*tert*-butyl)benzylidene)-5,5,8a-trimethyl-2-methylene-6-oxodecahydronaphthalen-1-yl) methoxy)-2*H*-chromen-2-one (3g). Yellow powder, yield: 87%; m.p.: 121 °C. NMR ^{1}H ($CDCl_3$, 600 MHz) δ_H: 7.66 (1H, d, J = 9.5 Hz, H-4), 7.56 (1H, d, J = 1.9 Hz, H-7″), 7.42 (1H, d, J = 8.3 Hz, H-5), 7.42 (2H, d, J = 8.3 Hz, H-2″,6″), 7.37 (1H, d, J = 8.5 Hz, H-3″,5″), 6.90 (1H, dd, J = 8.4; 2.4 Hz, H-6), 6.89 (1H, d, J = 2.3 Hz, H-8), 6.28 (1H, d, J = 9.5 Hz, H-3), 4.98 (1H, s, H-12′a), 4.55 (1H, s, H-12′b), 4.26 (1H, dd, J = 9.9; 5.8 Hz, H-11′a), 4.23 (1H, dd, J = 9.9; 5.9 Hz, H-11′b), 3.24 (1H, dd, J = 16.4; 0.7 Hz, H-1′a), 2.77 (1H, dd, J = 16.4; 2.7 Hz, H-1′b), 2.51 (1H, m, H-7′a), 2.50 (1H, m, H-9′), 2.18 (1H, td, J = 12.9; 4.3 Hz, H-7′b), 1.93 (1H, dd, J = 12.7; 3.5 Hz, H-5′), 1.80 (1H, dq, J = 13.0; 3.8 Hz, H-6′a), 1.52 (1H, qd, J = 13.1; 4.2 Hz, H-6′b), 1.28 (9H, s, H-9″,10″,11″), 1.20 (3H, s, H-13′), 1.17 (3H, s, H-14′), 0.77 (3H, s, H-15′). NMR ^{13}C ($CDCl_3$, 150 MHz) δ_C:206.7 (C-3′), 161.8 (C-7), 161.0 (C-2), 156.1 (C-9), 152.3 (C-4″), 146.2 (C-8′), 143.7 (C-4), 137.9 (C-7″), 132.7 (C-1″), 132.0 (C-2′), 130.6 (C-2″,6″), 125.8 (C-3″,5″), 129.2 (C-5), 113.6 (C-3), 112.9 (C-6), 112.6 (C-10), 108.2 (C-12′), 101.9 (C-8), 66.4 (C-11′), 53.0 (C-9′), 52.4 (C-5′), 45.5 (C-4′), 42.2 (C-1′), 38.9 (C-10′), 37.6 (C-7′), 34.6 (C-8″), 31.2 (C-9″,10″,11″), 30.3 (C-13′), 26.4 (C-6′), 23.0 (C-14′), 14.0 (C-15′). ESI-HRMS $[M + H]^+$ calcd. for $[C_{35}H_{41}O_4]^+$: 525.30048, found: 525.30090.

3.5.8 7-(((1R,4aS,8aR)-7-((*E*)-4-methoxybenzylidene)-5,5,8a-trimethyl-2-methylene-6-oxodecahydronaphthalen-1-yl) methoxy)-2*H*-chromen-2-one (3h). Yellow powder, yield: 81%; m.p.: 117 °C. NMR ^{1}H ($CDCl_3$, 600 MHz) δ_H: 7.66 (1H, d, J = 9.5 Hz, H-4), 7.55 (1H, d, J = 1.8 Hz, H-7″), 7.45 (2H, d, J = 8.3 Hz, H-2″,6″), 7.42 (1H, d, J = 8.8 Hz, H-5), 6.90 (1H, m, H-3″,5″), 6.90 (1H, m, H-6), 6.89 (1H, d, J = 2.4 Hz, H-8), 6.28 (1H, d, J = 9.5 Hz, H-3), 4.98 (1H, s, H-12′a), 4.56 (1H, s, H-12′b), 4.26 (1H, dd, J = 8.9; 4.9 Hz, H-11′a), 4.25 (1H, dd, J = 8.8; 4.7 Hz, H-11′b), 3.82 (3H, s, H-8″). 3.22 (1H, d, J = 16.2 Hz, H-1′a), 2.75 (1H, dd, J = 16.3; 2.6 Hz, H-1′b), 2.51 (1H, m, H-7′a), 2.50 (1H, t, J = 5.0 Hz, H-9′), 2.18 (1H, td, J = 13.0; 4.2 Hz, H-7′b), 1.92 (1H, dd, J = 12.7; 3.5 Hz, H-5′), 1.80 (1H, dq, J = 12.8; 3.6 Hz, H-6′a), 1.53 (1H, qd, J = 13.2; 4.1 Hz, H-6′b), 1.19 (3H, s, H-13′), 1.17 (3H, s, H-14′), 0.78 (3H, s, H-15′). NMR ^{13}C ($CDCl_3$, 150 MHz) δ_C:206.8 (C-3′), 161.9 (C-7), 161.1 (C-2), 160.2 (C-4″), 156.1 (C-9), 146.1 (C-8′), 143.7 (C-4), 137.8 (C-7″), 132.5 (C-1″), 130.7 (C-2′), 132.6 (C-2″,6″), 129.1 (C-5), 113.9 (C-3″,5″), 113.6 (C-3), 113.3 (C-6), 112.9 (C-10), 108.3 (C-12′), 101.8 (C-8), 66.3 (C-11′), 55.5 (C-8″), 53.0 (C-9′), 52.7 (C-5′), 45.5 (C-4′), 42.3 (C-1′), 38.9 (C-10′), 37.5 (C-7′), 30.3 (C-13′), 26.4 (C-6′), 23.0 (C-14′), 14.0 (C-15′). ESI-HRMS $[M + H]^+$ calcd. for $[C_{32}H_{35}O_5]^+$: 499.24845, found: 499.24875.

3.5.9 7-(((1R,4aS,8aR)-7-((*E*)-2-methoxybenzylidene)-5,5,8a-trimethyl-2-methylene-6-oxodecahydronaphthalen-1-yl) methoxy)-2*H*-chromen-2-one (3i). Yellow powder, yield: 72%; m.p.: 80 °C. NMR ^{1}H ($CDCl_3$, 600 MHz) δ_H: 7.84 (1H, d, J = 2.6 Hz, H-7″), 7.66 (1H, d, J = 9.5 Hz, H-4), 7.37 (1H, d, J = 8.8 Hz, H-5), 7.31 (2H, m, H-4″,6″), 6.90 (2H, m, H-3″,5″), 6.80 (1H, dd, J = 8.5; 2.4 Hz, H-6), 6.79 (1H, d, J = 2.3 Hz, H-8), 6.28 (1H, d, J = 9.5 Hz, H-3), 4.96 (1H, s, H-12′a), 4.53 (1H, s, H-12′b), 4.21 (1H, dd, J = 9.9; 6.4 Hz, H-11′a), 4.17 (1H, dd, J = 9.9; 5.3 Hz, H-11′b), 3.84 (3H, s, H-8″), 3.18 (1H, d, J = 16.0 Hz, H-1′a), 2.65 (1H, dd, J = 15.9; 2.9 Hz, H-1′b), 2.50 (1H, ddd, J = 12.8; 3.9; 2.8 Hz, H-7′a), 2.44 (1H, t, J = 5.7 Hz, H-9′), 2.15 (1H, td, J = 13.1; 4.2 Hz, H-7′b), 1.90 (1H, dd, J = 12.7; 3.4 Hz, H-5′), 1.80 (1H, dq, J = 12.9; 4.2 Hz, H-6′a), 1.52 (1H, qd, J = 13.2; 4.2 Hz, H-6′b), 1.22 (3H, s, H-13′), 1.16 (3H, s, H-14′), 0.78 (3H, s, H-15′). NMR ^{13}C ($CDCl_3$, 150 MHz) δ_C:206.6 (C-3′), 162.1 (C-7), 161.4 (C-2), 156.1 (C-9), 146.1 (C-8′), 143.6 (C-4), 133.8 (C-7″), 132.6 (C-1″), 132.7 (C-2′), 130.4 (C-4″), 130.1 (C-6″), 129.0 (C-5), 120.1 (C-5″), 113.6 (C-3), 113.3 (C-6), 112.8 (C-10), 110.9 (C-3″), 108.3 (C-12′), 101.8 (C-8), 66.1 (C-11′), 55.5 (C-8″), 53.1 (C-5′), 52.9 (C-9′), 45.8 (C-4′), 41.7 (C-1′), 39.0 (C-10′), 37.6 (C-7′), 29.9 (C-13′), 26.2 (C-6′), 23.2 (C-14′), 14.0 (C-15′). ESI-HRMS $[M + H]^+$ calcd. for $[C_{32}H_{35}O_5]^+$: 499.24845, found: 499.24857.

3.5.10 7-(((1R,4aS,8aR)-7-((*E*)-3,4-dimethoxybenzylidene)-5,5,8a-trimethyl-2-methylene-6-oxodecahydronaphthalen-1-yl) methoxy)-2*H*-chromen-2-one (3j). Yellow powder, yield: 75%; m.p.: 76 °C. NMR ^{1}H ($CDCl_3$, 600 MHz) δ_H: 7.65 (1H, d, J = 9.5 Hz, H-4), 7.54 (1H, d, J = 1.7 Hz, H-7″), 7.41 (1H, d, J = 8.5 Hz, H-5), 7.13 (1H, dd, J = 8.4, 1.8 Hz, H-6″), 6.96 (1H, d, J = 1.9 Hz, H-2″), 6.89 (1H, d, J = 8.2 Hz, H-5″), 6.88 (1H, d, J = 1.8 Hz, H-8), 6.87 (1H, dd, J = 8.6; 2.3 Hz, H-6), 6.28 (1H, d, J = 9.5 Hz, H-3), 4.99 (1H, s, H-12′a), 4.58 (1H, s, H-12′b), 4.28 (1H, dd, J = 10.0; 6.4 Hz, H-11′a), 4.25 (1H, dd, J = 10.0; 5.5 Hz, H-11′b), 3.88 (3H, s, H-9″), 3.83 (3H, s, H-8″), 3.28 (1H, dd, J = 16.2; 0.7 Hz, H-1′a), 2.74 (1H, dd, J = 16.3; 2.6 Hz, H-1′b), 2.52 (1H, ddd, J = 12.9; 3.9; 2.7 Hz, H-7′a), 2.49 (1H, m, H-9′), 2.17 (1H, td, J = 12.8; 3.6 Hz, H-7′b), 1.93 (1H, dd, J = 12.7; 3.5 Hz, H-5′), 1.80 (1H, m, H-6′a), 1.54 (1H, qd, J = 13.2; 4.0 Hz, H-6′b), 1.20 (3H, s, H-13′), 1.18 (3H, s, H-14′), 0.78 (3H, s, H-15′). NMR ^{13}C ($CDCl_3$, 150 MHz) δ_C:206.8 (C-3′), 162.1 (C-7), 161.2 (C-2), 156.1 (C-9), 149.8 (C-4″), 149.0 (C-3″), 146.1 (C-8′), 143.7 (C-4), 138.1 (C-7″), 131.1 (C-2′), 129.2 (C-5), 128.6 (C-1″), 123.3 (C-6″), 114.5 (C-2″), 113.6 (C-3), 112.9 (C-6), 112.8 (C-10), 111.2 (C-5″), 108.5 (C-12′), 101.6 (C-8), 66.3 (C-11′), 56.0 (C-9″), 55.9 (C-8″), 53.1 (C-9′), 52.7 (C-5′), 45.6 (C-4′), 42.1 (C-1′), 38.8 (C-10′), 37.5 (C-7′), 30.0 (C-13′), 26.4 (C-6′), 23.0 (C-14′), 14.1 (C-15′). ESI-HRMS $[M + H]^+$ calcd. for $[C_{33}H_{37}O_6]^+$: 529.25901, found: 529.25928.

3.5.11 7-(((1R,4aS,8aR)-5,5,8a-trimethyl-2-methylene-6-oxo-7-((*E*)-3-(1,1,2,2-tetrafluoroethoxy)benzylidene)decahydronaphthalen-1-yl)methoxy)-2*H*-chromen-2-one (3k). Yellow powder, yield: 89%; m.p.: 69 °C. NMR ^{1}H ($CDCl_3$, 600 MHz) δ_H: 7.65 (1H, d, J = 9.5 Hz, H-4), 7.52 (1H, d, J = 2.1 Hz, H-7″), 7.38 (1H, t, J = 7.9 Hz, H-5″), 7.37 (1H, d, J = 8.5 Hz, H-5), 7,34 (1H, d, J = 7.8 Hz, H-6″), 7.28 (1H, s, H-2″), 7.18 (1H, dd, J = 8.1; 0.8 Hz, H-4″), 6.83 (1H, dd, J = 8.5; 2.4 Hz, H-6), 6.82 (1H, d, J = 2.3 Hz, H-8), 6.28 (1H, d, J = 9.5 Hz, H-3), 5.90 (1H, tt, J = 53.0; 2.6 Hz, H-9″), 5.00 (1H, s, H-12′a), 4.58 (1H, s, H-12′b), 4.24 (1H, dd, J = 9.8; 6.5 Hz, H-11′a), 4.20 (1H, dd, J = 9.8; 5.2 Hz, H-11′b), 3.24 (1H, d, J = 16.2 Hz, H-1′a), 2,70 (1H, dd, J = 16.2; 2.7 Hz, H-1′b), 2.53 (1H, m, H-7′a), 2.47 (1H, t, J = 5.7 Hz, H-9′), 2.17 (1H, td, J = 13.0; 4.1 Hz, H-7′b), 1.92 (1H, dd, J = 12.7; 3.4 Hz, H-5′), 1.80 (1H, dq, J = 12.9; 3,7 Hz, H-6′a), 1.55 (1H, qd, J = 13.2; 4.2 Hz, H-6′b), 1.22 (3H, s, H-13′), 1.18 (3H, s, H-14′), 0.80 (3H, s, H-15′). NMR ^{13}C ($CDCl_3$, 150 MHz) δ_C:206.8 (C-3′), 161.8 (C-7), 161.1 (C-2), 155.9 (C-9), 149.0 (C-3″), 145.7 (C-8′), 143.6 (C-4), 137.6 (C-1″), 136.3 (C-7″), 134.8 (C-2′), 130.5 (C-5″), 129.8 (C-8″), 129.0 (C-5), 128.6 (C-6″), 123.1 (C-2″), 122.0 (C-4″), 113.5 (C-3), 113.0 (C-6), 112.9 (C-10), 112.7 (C-9″), 108.6 (C-12′), 101.7 (C-8), 66.1 (C-11′), 53.0 (C-5′), 52.9 (C-9′), 45.7 (C-4′), 41.6 (C-1′), 39.0 (C-10′), 37.4 (C-7′), 29.9 (C-13′), 26.2 (C-6′), 23.1 (C-14′), 14.1 (C-15′). ESI-HRMS $[M + H]^+$ calcd. for $[C_{33}H_{33}F_4O_5]^+$: 585.22641, found: 585.22647.

3.5.12 7-(((1R,4aS,8aR)-7-((*E*)-4-(dimethylamino)benzylidene)-5,5,8a-trimethyl-2-methylene-6-oxodecahydronaphthalen-1-yl)methoxy)-2*H*-chromen-2-one (3l). Yellow powder, yield: 78%; m.p.: 150 °C. NMR ^{1}H ($CDCl_3$, 600 MHz) δ_H: 7.65 (1H, d, J = 9.5 Hz, H-4), 7.57 (1H, d, J = 1.7 Hz, H-7″), 7.43 (2H, d, J = 8.4 Hz, H-2″,6″), 7.42 (1H, d, J = 7.8 Hz, H-5), 6.93 (1H, d, J = 2.4 Hz, H-8), 6.92 (1H, m, H-6), 6.66 (2H, d, J = 8.9 Hz, H-3″,5″), 6.27 (1H, d, J = 9.5 Hz, H-3), 4.97 (1H, s, H-12′a), 4.55 (1H, s, H-12′b), 4.29 (1H, m, H-11′), 3.23 (1H, d, J = 15.7 Hz, H-1′a), 2.99 (6H, s, H-8″,9″), 2.77 (1H, dd, J = 16.1; 2.4 Hz, H-1′b), 2.51 (1H, m, H-7′a), 2.51 (1H, t, J = 5.4 Hz, H-9′), 2.17 (1H, td, J = 12.9; 4.1 Hz, H-7′b), 1.91 (1H, dd, J = 12.7; 3.5 Hz, H-5′), 1.80 (1H, dq, J = 13.0; 3.9 Hz, H-6′a), 1.52 (1H, qd, J = 13.1; 4.2 Hz, H-6′b), 1.18 (3H, s, H-13′), 1.17 (3H, s, H-14′), 0.78 (3H, s, H-15′). NMR ^{13}C ($CDCl_3$, 150 MHz) δ_C:206.4 (C-3′), 162.1 (C-7), 161.2 (C-2), 150.6 (C-4″), 156.1 (C-9), 146.4 (C-8′), 143.7 (C-4), 139.2 (C-7″), 132.9 (C-2″,6″), 129.2 (C-5), 127.8 (C-2′), 123.5 (C-1″), 113.5 (C-3), 112.9 (C-6), 112.7 (C-10), 111.9 (C-3″,5″), 108.1 (C-12′), 102.2 (C-8), 66.4 (C-11′), 53.1 (C-9′), 52.6 (C-5′), 45.2 (C-4′), 42.6 (C-1′), 40.3 (C-8″,9″), 38.8 (C-10′), 37.7 (C-7′), 30.4 (C-13′), 26.5 (C-6′), 23.0 (C-14′), 14.0 (C-15′). ESI-HRMS $[M + H]^+$ calcd. for $[C_{33}H_{38}NO_4]^+$: 512.28008, found: 512.27966.

3.5.13 7-(((1R,4aS,8aR)-5,5,8a-trimethyl-2-methylene-6-oxo-7-((*E*)-4-(pyrrolidin-1-yl)benzylidene)decahydronaphthalen-1-yl) methoxy)-2*H*-chromen-2-one (3m). Yellow powder, yield: 74%; m.p.: 150 °C. NMR ^{1}H ($CDCl_3$, 600 MHz) δ_H: 7.66 (1H, d, J = 9.5 Hz, H-4), 7.59 (1H, d, J = 1.7 Hz, H-7″), 7.43 (2H, d, J = 8.8 Hz, H-2″,6″), 7.42 (1H, d, J = 8.4 Hz, H-5), 6.93 (1H, m, H-6), 6.91 (1H, d, J = 2.4 Hz, H-8), 6.52 (2H, d, J = 8.8 Hz, H-3″,5″), 6.27 (1H, d, J = 9.5 Hz, H-3), 4.97 (1H, s, H-12′a), 4.55 (1H, s, H-12′b), 4.29 (1H, dd, J = 8.3; 4.3 Hz, H-11′a), 4.26 (1H, dd, J = 8.4; 4.5 Hz, H-11′b), 3.29 (4H, m, H-2‴,5‴), 3.22 (1H, d, J = 16.2 Hz, H-1′a), 2.76 (1H, dd, J = 16.1; 2.0 Hz, H-1′b), 2.52 (1H, m, H-9′), 2.50 (1H, m, H-7′a), 2.17 (1H, td, J = 13.0; 4.1 Hz, H-7′b), 2.01 (4H, m, H-3‴,4‴), 1.91 (1H, dd, J = 12.7; 3.4 Hz, H-5′), 1.80 (1H, dq, J = 13.2; 3.8 Hz, H-6′a), 1.52 (1H, qd, J = 13.2; 4.1 Hz, H-6′b), 1.18 (3H, s, H-13′), 1.17 (3H, s, H-14′), 0.78 (3H, s, H-15′). NMR ^{13}C ($CDCl_3$, 150 MHz) δ_C:206.4 (C-3′), 162.2 (C-7), 161.3 (C-2), 156.1 (C-9), 148.3 (C-4″), 146.6 (C-8′), 143.7 (C-4), 139.6 (C-7″), 133.1 (C-2″,6″), 129.2 (C-5),

127.2 (C-2′), 122.9 (C-1″), 113.5 (C-3), 112.6 (C-6), 111.7 (C-10), 111.7 (C-3″,5″), 108.0 (C-12′), 102.3 (C-8), 66.4 (C-11′), 53.2 (C-9′), 52.6 (C-5′), 47.6 (C-2‴,5‴), 47.6 (C-4′), 42.7 (C-1′), 38.8 (C-10′), 37.7 (C-7′), 30.2 (C-13′), 26.5 (C-6′), 25.6 (C-3‴,4‴), 23.0 (C-14′), 14.0 (C-15′). ESI-HRMS $[M + H]^+$ calcd. for $[C_{35}H_{40}NO_4]^+$: 538.29573, found: 538.29531.

3.6. α-Amylase inhibition and kinetics Assay

Anti-α-amylase activity was evaluated according to the protocol reported in the literature with slight modifications.[36] First, 500 μL of diluted α-amylase from porcine pancreas (1151 U mg^{-1} of protein: 480 μL of amylase in 0.2 mol L^{-1} phosphate buffer, pH = 6) and 500 μL of soluble starch solution (1%). To evaluate this activity, the effects of each of the synthesized compounds, the solutions of diluted α-amylase and the different concentrations of compound (6.25–50 μM) were preincubated at 25 °C for 5 min. To start the reaction, 500 μL of substrate (soluble starch) was added to solutions and incubated for 10 min at 25 °C. Finally, 3 mL of 3,5-dinitrosalicylic acid (DNS) was quickly added to the mixture and heated in boiling water for 15 min. Glucose was used to schematize a standard curve. Acarbose was used as the positive control. The absorbance was measured at 540 nm. The increased substrate concentration (from 0.5 to 2.5%) was tested by kinetic analysis to determine the inhibition type exerted on α-amylase (competitive, non-competitive, mixed or uncompetitive) by the line Weaver–Burk plot.

3.7. Molecular docking procedure

The chemical structures of all molecules were sketched and optimized using the ACD software (3D Viewer) (**http://www.filefacts.com/acd3d-viewer-freeware-info**). The 3D-structure of *Aspergillus oryzae* α-amylase complexed with acarbose (7TAA.pdb) was retrieved from RCSB PDB, Protein Data Bank website (**https://www.rcsb.org/**). Python Molecule Viewer (version 1.5.6rc3) was employed for enzyme optimization and simplification, by removing water molecules and the co-crystallized inhibitor (acarbose) from the protein file, and then protonated by adding polar hydrogens. Kollman charges were inserted. All structures were saved in PDBQT file format before running the docking using the AutoDock Vina software.[37] Hence, for the competitive-type inhibitors, the molecular docking launch was performed in the grid box centered on the enzymatic 3D-structure with the following coordinates: 38.725, 44.127, 25.633 (x, y, z), a spacing of 0.375 Å and a box size of 65 × 52 × 52.[28] These parameters, together with the enzyme and ligand pdbqt files and the number of modes (9), were included in the configuration file. The exhaustiveness value was fixed to 8. For the uncompetitive and noncompetitive-type inhibitors, the whole protein was selected as a binding site to dock the selected ligands. The BIOVIA Discovery Studio Visualizer (2017) (BIOVIA, D. S., version 17.2.0.16349) was used to visualize the molecule-enzyme interactions and generate Figures.

3.8. Statistical analysis

GraphPad Prism 7.0 (Graph Pad Software Inc., CA and USA) was used to conduct the statistical analysis. The results are given as mean values ± standard deviation (SD). Tukey's test was applied to determine the difference between the activities of all compounds.

4 Conclusions

The natural bioactive coladonin **1** isolated quantitatively from the roots of the Tunisian endemic plant *F. tunetana* has been oxidized and condensed with different aryl aldehydes *via* the Claisen–Schmidt reaction to obtain a series of new arylidene-based coladonin conjugates. All synthetic derivatives were evaluated for their potential α-amylase inhibitory activity. The compounds **3k** and **3m** with a more interesting activity than that of acarbose were used as the standard. Kinetic studies have shown that these compounds act as mixed inhibitors towards α-amylase. From the molecular docking analysis, it can be concluded that the arylidene moiety is essential for the buildup and enhancement of α-amylase inhibitory activity of compounds **3a–m**. *In silico* "SAR" studies were found to be in good agreement with the experimental biological results, showing that the nature of the arylidene moiety is essential to form several important binding interactions with the amino acids of the enzyme. Thus, these arylidene-based coladonin derivatives as valuable candidates may serve as lead for the future development of potential anti-diabetic agents.

Author contributions

Wiem Baccari, Ilyes Saidi and Mansour Znati: investigation, methodology, software, writing – original draft. Houda Lazrag, Axel Marchal, Pierre Waffo-Teguo: validation, supervision and conceptualization. Insaf Filali and Moncef Tounsi: visualization. Hichem Ben Jannet: supervision, validation, reviewing and editing.

Conflicts of interest

There are no conflicts to declare.

Acknowledgements

This study is supported *via* funding from Prince sattam bin Abdulaziz University project number (PSAU/2023/R/1444). The authors are grateful to Researchers Supporting Project number (PSAU/2023/R/1444) at Prince sattam bin Abdulaziz University, Saudi Arabia.

References

1 M. A. B. Khan, M. J. Hashim, J. K. King, R. D. Govender, H. Mustafa and J. Al Kaabi, *J. Epidemiol. Glob. Health*, 2000, **10**, 107–111.

2 M. E. Febrian, F. X. Ferdinan, G. P. Sendani, K. M. Suryanigrum and R. Yunanda, *Procedia Comput. Sci.*, 2023, **216**, 21–30.
3 C. Lo, T. Toyama, Y. Wang, J. Lin, Y. Hirakawa, M. Jun, A. Cass, C. M. Hawley, H. Pilmore and S. V. Badve, *Cochrane Database Syst. Rev.*, 2018, **9**, CD011798.
4 J. Dowarah and V. P. Singh, *Bioorg. Med. Chem.*, 2020, **28**, 115263.
5 S. Khan, M. Khan, W. Rehman, M. Shah, R. Hussain, L. Rasheed, Y. Khan, A. Dera, R. Pashameah and E. Alzahrani, *Pharmaceuticals*, 2022, **15**, 1164–1180.
6 H. Gin and V. Rigalleau, *Diabetes Metab.*, 2000, **26**, 265–272.
7 N. Kaur, V. Kumar, S. K. Nayak, P. Wadhwa, P. Kaur and S. K. Sahu, *Chem. Biol. Drug Des.*, 2021, **98**, 539–560.
8 J. Wang, X. Rong, W. Li, Y. Yang, J. Yamahara and Y. Li, *J. Ethnopharmacol.*, 2012, **142**, 782–788.
9 J. P. Nie, Z. N. Qu, Y. Chen, J. H. Chen, Y. Jiang, M. N. Jin, Y. Yu, W. Y. Niu, H. Q. Duan and N. Qin, *Fitoterapia*, 2020, **142**, 104499.
10 H. Kashtoh and K. H. Baek, *Plants*, 2023, **12**, 2944.
11 M. Znati, I. Filali, A. Jabrane, J. Casanova and H. Ben Jannet, *Chem. Biodiversity*, 2017, **14**, e1600116.
12 F. U. Afifi and B. Abu-Irmaileh, *J. Ethnopharmacol.*, 2000, **72**, 101–110.
13 G. Pottier-Alapetite, *'Flore de la Tunisie, AngiospermesDicotyledones, Apetales-Dialypetales'*, Publications Scientifiques Tunisiennes, Imprimerie Officielle de la Republique Tunisienne, Tunisie, 1979, p. 607.
14 A. Jabrane, O. Duchamp, H. Ben Jannet, Z. Mighri, J. F. Mirjolet, F. Harzallah-Skhiri and M. A. Lacaille-Dubois, *Chem. Biodiversity*, 2010, **7**, 392–399.
15 M. Curini, G. Cravotto, F. Epifano and G. Giannone, *Curr. Med. Chem.*, 2006, **13**, 199–222.
16 I. Choudhary, M. I. Baig and M. Nur-e-Alam, *Helv. Chim. Acta*, 2001, **84**, 2409–2416.
17 A. Amin, M. Hanif, A. Rafey, S. Zaib, S. Bakhsh, M. Ramzan, A. Zaman, F. Ur Rehman, J. Iqbal and L. Pieters, *Rev. Bras. Farmacogn.*, 2020, **30**, 12–17.
18 A. V. Petrova, E. F. Khusnutdinova, A. N. Lobov, L. M. Zakirova, N. T. T. Ha and D. A. Babkov, *Nat. Prod. Res.*, 2022, **36**, 1–8.
19 V. Kumar, R. Ramu, P. S. Shirahatti, V. B. C. Kumari, P. Sushma, S. P. Mandal and S. M. Patil, *ChemistrySelect*, 2021, **6**, 9637–9644.
20 D. Kumar, S. Narwal and J. S. Sandhu, *Int. J. Med. Chem.*, 2013, **2013**, 1–4.
21 S. W. Kahssay, G. S. Hailu and K. T. Desta, *Drug Des., Dev. Ther.*, 2021, **15**, 3119–3129.
22 S. Saouli, I. Selatnia, B. Zouchoune, A. Sid, S. M. Zendaoui, C. Bensouici and E. Bendeif, *J. Mol. Struct.*, 2020, **1213**, 128203.
23 S. Farooq and Z. Ngaini, *ChemistrySelect*, 2020, **5**, 9974–9979.
24 K. Kaleshkumar, R. Rajaram, N. Gayathri, T. Sivasudha, G. Arun, G. Archunan, B. Gulyas and P. Padmanabhan, *Bioorg. Chem.*, 2019, **90**, 103072.
25 V. B. Nguyen, A. D. Nguyen, Y. H. Kuo and S. L. Wang, *Int. J. Mol. Sci*, 2017, **18**, 700–711.
26 B. Somashekara, B. Thippeswamy and G. R. Vijayakumar, *J. Chem. Sci.*, 2019, **131**, 1–7.
27 M. Nawaz, M. Taha, F. Qureshi, N. Ullah, M. Selvaraj, S. Shahzad, S. Chigurupati, A. Waheed and F. A. Almutairi, *BMC Chem.*, 2020, **14**, 43–53.
28 I. Saidi, M. Manachou, M. Znati, J. Bouajila and H. Ben Jannet, *J. Mol. Struct.*, 2022, **1247**, 131379.
29 I. Ul Haq, M. Ahmad, I. Ali, K. M. Khan, S. Chigurupati, A. Habib, U. Sala, S. Konanki, S. G. Felemban, M. Taha and Z. Ul Haq, *Chem. Pap.*, 2023, **77**, 2581–2604.
30 E. S. H. El Ashry, M. M. K. Farahat, L. F. Awad, M. Balbaa, H. Yusef, M. E. I. Badawy and M. N. Abd Al Moaty, *J. Mol. Struct.*, 2022, **1259**, 132733.
31 W. Baccari, I. Saidi, M. Znati, A. M. Mustafa, G. Caprioli, A. H. Harrath and H. Ben Jannet, *Process Biochem.*, 2023, **129**, 230–240.
32 F. K. Algethami, I. Saidi, H. N. Abdelhamid, M. R. Elamin, B. Y. Abdulkhair, A. Chrouda and H. Ben Jannet, *Molecules*, 2021, **26**, 5214–5231.
33 E. O. Yeye, K. M. Khan, S. Chigurupati, A. Wadood, A. U. Rehman, S. Perveen and M. Taha, *Bioorg. Med. Chem*, 2020, **28**, 115467.
34 W. D. Duan, J. Y. Cao, C. Y. Cai, Z. R. Yang, J. F. Cui, T. Lan and B. Wang, *J. Mol. Struct.*, 2022, **1263**, 133026.
35 Y. Yang, Q. Zhu, Y. Zhong, X. Cui, Z. Jiang, P. Wu and S. Zhao, *Bioorg. Chem.*, 2020, **101**, 103985.
36 A. Assel, A. Hajlaoui, H. Lazrag, M. Manachou, A. Romdhane, J. Kraiem and H. Ben Jannet, *J. Mol. Struct.*, 2023, **1271**, 134020.
37 O. Trott and A. J. Olson, *J. Comput. Chem.*, 2010, **31**, 455–461.